doi:10.3772/j.issn.1006-6748.2019.04.011

Adaptive fuzzy compensation based composite nonlinear feedback controller design for robot manipulators①

Jiang Yuan(蒋 沅)* **, Gong Chenglong②*, Dai Jiyang*
(* College of Information Engineering, Nanchang Hangkong University, Nanchang 330063, P. R. China)
(** School of Engineering Science, University of Chinese Academy of Sciences, Beijing 100049, P. R. China)

Abstract

In order to suppress the influence of uncertain factors on robot system and enable an uncertain robot system to track the reference input accurately, a strategy of combining composite nonlinear feedback (CNF) control and adaptive fuzzy control is studied, and a robot CNF controller based on adaptive fuzzy compensation is proposed. The key of this strategy is to use adaptive fuzzy control to approach the uncertainty of the system online, as the compensation term of the CNF controller, and make full use of the advantages of the two control methods to reduce the influence of uncertain factors on the performance of the system. The convergence of the closed-loop system is proved by feedback linearization and Lyapunov theory. The final simulation results confirm the effectiveness of this plan.

Key words: robot, uncertainty, composite nonlinear feedback (CNF), adaptive fuzzy control, system convergence

0 Introduction

Trajectory tracking is a basic task for robot control[1]. The main control objective is to design the controller, track the reference trajectory periodically, and make the robot manipulators track the reference trajectory asymptotically. There are numerous control methods for robots[2-7], which mainly include calculation of torque control, adaptive control, optimal control, robust control, fuzzy control, neural networks control, etc. Ref. [8] proposed an efficient implementation of robust controller on 3-DOF parallel robot driven by pneumatic muscle actuators (PMAs). Based on multiple model adaptive control method, Ref. [9] presented a new algorithm for calculating the control-weight aiming at the problem that great change in parameters always leads to large transient error. Ref. [10] presented the Mamdami fuzzy control logic to overcome the motion control of multi-DOF TWIP robot and make its motion smooth and steady control. A fuzzy NN learning algorithm was developed in Ref. [11] to identify the uncertain plant model. And the prominent feature of the fuzzy NN is that there is no need to get the prior knowledge about the uncertainty and a sufficient amount of observed data. Ref. [12] developed an adaptive controller with a fuzzy tuner for a cable-based rehabilitation robot. And the fuzzy tuner can adjust the control parameters according to position error and the change of error, thus the time-varying control parameters can be optimized by this tuner. Ref. [13] presented an adaptive fuzzy logic modeling and control of two link robot manipulator with uncertainties.

Composite nonlinear feedback[14] (CNF) is a computed torque control theory that can be used as an effective method to perform set point tracking tasks of saturated systems. Ref. [15] verified that the composite feedback control performance was better than the time optimal control in terms of set point tracking tasks. However, when there is disturbance in the system or the system model is not accurate (hereinafter referred to as uncertainty), the system under the control of CNF would be no longer able to match the reference input accurately.

If the uncertain model is known, control compensation can be applied to the system to offset the uncer-

① Supported by the National Natural Science Foundation of China (No. 61663030, 61663032), Natural Science Foundation of Jiangxi Province (No. 20142BAB207021), the Foundation of Jiangxi Educational Committee (No. GJJ150753), the Innovation Fund Designated for Graduate Students of Nanchang Hangkong University (No. YC2017027), the Open Fund of Key Laboratory of Image Processing and Pattern Recognition of Jiangxi Province (Nanchang Hangkong University) (No. TX201404003), Key Laboratory of Nondestructive Testing (Nanchang Hangkong University), Ministry of Education (No. ZD29529005), and the Reform Project of Degree and Postgraduate Education in Jiangxi (No. JXYJG-2017-131).
② To whom correspondence should be addressed. E-mail: 13791257790@163.com
Received on Oct. 10, 2018

tainty of each instant, and the effect of uncertainty on the performance of the system can be eliminated, which is model-based compensation. However, it is impossible to establish an accurate mathematical model of uncertainty and completely compensate for the effects of uncertainty based on the mathematical model.

This paper uses an adaptive fuzzy control system[16] with fuzzy generator and fuzzy eliminator to estimate the uncertainty online and uses the estimated result as a compensation term of CNF controller to design a new CNF controller based on adaptive fuzzy compensation. The new controller can reduce the impact of uncertainty on the system, and make the system obtain stronger stability and robustness.

1 Problem formulation and adaptive fuzzy control

The equations of motion of an n-link rigid robot can be expressed as

$$\boldsymbol{M}(\boldsymbol{q})\ddot{\boldsymbol{q}} + \boldsymbol{C}(\boldsymbol{q},\dot{\boldsymbol{q}})\dot{\boldsymbol{q}} + \boldsymbol{G}(\boldsymbol{q}) = \boldsymbol{\tau} + \boldsymbol{F}(\boldsymbol{q},\dot{\boldsymbol{q}},\ddot{\boldsymbol{q}}) \quad (1)$$

where $\boldsymbol{M}(\boldsymbol{q})$ is an $n \times n$ inertia matrix, which is a positive definite matrix, $\boldsymbol{C}(\boldsymbol{q},\dot{\boldsymbol{q}})$ is an $n \times n$ matrix containing the centrifugal and Coriolis terms, $\boldsymbol{G}(\boldsymbol{q})$ is an $n \times 1$ vector containing gravitational torques, $\boldsymbol{\tau}$ is joint drive torques (or forces) and $\boldsymbol{F}(\boldsymbol{q}, \dot{\boldsymbol{q}},\ddot{\boldsymbol{q}})$ is an uncertainty term consisting of friction, disturbance and model uncertainty.

The robot dynamics equation has the following properties[17]:

$\boldsymbol{M}(\boldsymbol{q}) \in \boldsymbol{R}^{n\times n}$ is symmetric, bounded, and positive definite.

The matrix $\dot{\boldsymbol{M}}(\boldsymbol{q}) - 2\boldsymbol{C}(\boldsymbol{q},\dot{\boldsymbol{q}})$ is skew symmetric, $\dot{\boldsymbol{q}}^{\mathrm{T}}[\dot{\boldsymbol{M}}(\boldsymbol{q}) - 2\boldsymbol{C}(\boldsymbol{q},\dot{\boldsymbol{q}})]\dot{\boldsymbol{q}} = 0$.

In practice, the precise mathematical model of the robot system is difficult to be obtained, and the controller can only be designed based on the ideal robot nominal model[18]. The original CNF controller can be designed as

$$\boldsymbol{\tau} = sat[\boldsymbol{M}(\boldsymbol{q})[sat_h(\ddot{\boldsymbol{q}}_d - \boldsymbol{k}_v\dot{\boldsymbol{e}} - \boldsymbol{k}_p\boldsymbol{e} - \rho(e)\boldsymbol{B}^{\mathrm{T}}P\begin{bmatrix}\boldsymbol{e}\\ \dot{\boldsymbol{e}}\end{bmatrix})] + \boldsymbol{C}(\boldsymbol{q},\dot{\boldsymbol{q}})\dot{\boldsymbol{q}} + \boldsymbol{G}(\boldsymbol{q})] \quad (2)$$

which is a linear time-invariant closed-loop system. It is stabilized by linear feedback and has global asymptotic stability, where $sat(\cdot)$ is saturation function in the form of $sat(\boldsymbol{u}) = \mathrm{sign}(\boldsymbol{u})\min\{\boldsymbol{u}_{\max}, |\boldsymbol{u}|\}$, which can effectively overcome the chattering of the system, $sat_h(\cdot):\boldsymbol{R}^n \to \boldsymbol{R}^n$ is the saturation vector value function of each channel inside the robot; $\boldsymbol{q}_d$ is the desired position; $\boldsymbol{e} = \boldsymbol{q} - \boldsymbol{q}_d$, $\dot{\boldsymbol{e}} = \dot{\boldsymbol{q}} - \dot{\boldsymbol{q}}_d$ are the errors and their derivatives; $\rho(e)$ is nonlinear feedback function. In the above equation, when gain matrices $\boldsymbol{k}_p = diag(\alpha^2, \alpha^2)$, $\boldsymbol{k}_v = diag(2\alpha, 2\alpha)$, $\alpha > 0$ are diagonally positive definite matrices, the robot system can be decoupled; $\boldsymbol{B} = [0 \quad \boldsymbol{I}]^{\mathrm{T}}$; P is the solution of the Lyapunov equation.

Substituting Eq. (1) with Eq. (2) can be obtained as

$$sat_m(\ddot{\boldsymbol{e}} + \boldsymbol{k}_v\dot{\boldsymbol{e}} + \boldsymbol{k}_p\boldsymbol{e} + \boldsymbol{\rho}(\boldsymbol{e})\boldsymbol{B}^{\mathrm{T}}P\begin{bmatrix}\boldsymbol{e}\\ \dot{\boldsymbol{e}}\end{bmatrix}) = \boldsymbol{M}^{-1}(\boldsymbol{q})\boldsymbol{F}(\boldsymbol{q},\dot{\boldsymbol{q}},\ddot{\boldsymbol{q}}) \quad (3)$$

where $|sat_m(\cdot)| \geqslant |sat_h(\cdot)|$. This would allow exemption of vibrations for a closed-loop system with large uncertainties; $\boldsymbol{M}^{-1}(\boldsymbol{q})\boldsymbol{F}(\boldsymbol{q},\dot{\boldsymbol{q}},\ddot{\boldsymbol{q}}) = \boldsymbol{f}(\boldsymbol{x})$, where $\boldsymbol{x} = [\boldsymbol{e} \quad \dot{\boldsymbol{e}}]^{\mathrm{T}}$. According to Eq. (3), $\boldsymbol{f}(\boldsymbol{x})$ contains a saturation function already.

In practice, it is necessary to approach the uncertain items so as to compensate for the uncertainties. In this paper, an adaptive fuzzy control system is used to approach the uncertain model online.

The basic structure of the fuzzy logic system[19] consists of 4 parts: fuzzification, reasoning synthesis, fuzzy rule base and anti-fuzzification. Fuzzy logic rules are represented by IF-THEN inference rules:

$\boldsymbol{R}^j$ If $\boldsymbol{x}_1$ is $\boldsymbol{F}_1^j$ and $\boldsymbol{x}_2$ is $\boldsymbol{F}_2^j$ and ... and $\boldsymbol{x}_n$ is $\boldsymbol{F}_n^j$, then $\boldsymbol{y}$ is $\boldsymbol{G}^j$, $j = 1,2,\cdots,M$.

where $\boldsymbol{x} \in \boldsymbol{R}^n$ is the input of the fuzzy system, and $\boldsymbol{y} \in \boldsymbol{R}$ is the output of the fuzzy system. $\boldsymbol{F}_i^j$ and $\boldsymbol{G}^j$ are fuzzy sets. According to the single valued fuzzification, product operation and weighted average defuzzification, the fuzzy logic system can be expressed as

$$\boldsymbol{y} = \frac{\sum_{j=1}^{M}\bar{y}^j(\prod_{i=1}^{n}\mu_F(x_i))}{\sum_{j=1}^{M}\prod_{i=1}^{n}\mu_F(x_i)}, \text{ denote } \boldsymbol{\xi}_j = \frac{\prod_{i=1}^{n}\mu_F(x_i)}{\sum_{j=1}^{M}\prod_{i=1}^{n}\mu_F(x_i)}$$

where $\mu_F(\bar{y}^j)$ is a fuzzy membership function, $\bar{y}^j$ is the point where $\mu_F(\bar{y}^j)$ gets the maximum value.

Defining that $\boldsymbol{\theta} = [\bar{y}^1, \bar{y}^2, \cdots, \bar{y}^M]^{\mathrm{T}}$ represents the adaptive parameter vector of the fuzzy control system, and $\boldsymbol{\xi}(\boldsymbol{x}) = [\xi_1(x), \cdots, \xi_M(x)]^{\mathrm{T}}$ represents the fuzzy basis function vector. The fuzzy logic system can be written as

$$\boldsymbol{y}(\boldsymbol{x}) = \boldsymbol{\theta}^{\mathrm{T}}\boldsymbol{\xi}(\boldsymbol{x}) \quad (4)$$

Assumption Define $\boldsymbol{\varepsilon}$ as the optimal approximation error, i.e., $\boldsymbol{\varepsilon} = \boldsymbol{f}(\boldsymbol{x}) - \hat{\boldsymbol{f}}(\boldsymbol{x},\boldsymbol{\theta}^*)$, and there is an ideal adaptive fuzzy output $\hat{\boldsymbol{f}}(\boldsymbol{x},\boldsymbol{\theta}^*)$ for the upper bound of the optimal error $\boldsymbol{\varepsilon}_0$, i.e.:

$$\max \|\hat{\boldsymbol{f}}(\boldsymbol{x},\boldsymbol{\theta}^*) - \boldsymbol{f}(\boldsymbol{x})\| \leqslant \boldsymbol{\varepsilon}_0$$

where $\boldsymbol{f}(\boldsymbol{x}, \boldsymbol{\theta}^*) = \boldsymbol{\theta}^{*\mathrm{T}}\boldsymbol{\xi}(\boldsymbol{x})$, and $\boldsymbol{\theta}^* = \mathrm{argmin}_{\theta\in\beta(M_\theta)}\{\sup_{x\in\varphi(M_x)}\|\boldsymbol{f}(\boldsymbol{x}) - \hat{\boldsymbol{f}}(\boldsymbol{x},\boldsymbol{\theta})\|\}$, $\boldsymbol{\theta}^*$ is the $n \times n$ order matrix, which represents the best approximation parameter for $\boldsymbol{f}(\boldsymbol{x})$.

2 New CNF controller

The new control law can be designed as

$$\boldsymbol{\tau} = sat[\boldsymbol{M}(\boldsymbol{q})[sat_h(\ddot{\boldsymbol{q}}_d - \boldsymbol{k}_v\dot{\boldsymbol{e}} - \boldsymbol{k}_p\boldsymbol{e} - \boldsymbol{\rho}(\boldsymbol{e})\boldsymbol{B}^{\mathrm{T}}\boldsymbol{P}\begin{bmatrix}\boldsymbol{e}\\ \dot{\boldsymbol{e}}\end{bmatrix}) - \hat{\boldsymbol{f}}(\boldsymbol{x},\boldsymbol{\theta})] + \boldsymbol{C}(\boldsymbol{q},\dot{\boldsymbol{q}})\dot{\boldsymbol{q}} + \boldsymbol{G}(\boldsymbol{q})] \quad (5)$$

where $\hat{\boldsymbol{\theta}}$ is the estimate of $\boldsymbol{\theta}^*$, $\hat{\boldsymbol{f}}(\boldsymbol{x},\boldsymbol{\theta}) = \hat{\boldsymbol{\theta}}^{\mathrm{T}}\boldsymbol{\xi}(\boldsymbol{x})$.

According to Eqs(1), (3), (5),

$$sat_m(\ddot{\boldsymbol{e}} + \boldsymbol{k}_v\dot{\boldsymbol{e}} + \boldsymbol{k}_p\boldsymbol{e} + \boldsymbol{\rho}(\boldsymbol{e})\boldsymbol{B}^{\mathrm{T}}\boldsymbol{P}\begin{bmatrix}\boldsymbol{e}\\ \dot{\boldsymbol{e}}\end{bmatrix}) + \hat{\boldsymbol{f}}(\boldsymbol{x},\boldsymbol{\theta}) = \boldsymbol{f}(\boldsymbol{x}) \quad (6)$$

and

$$\begin{aligned}\boldsymbol{f}(\boldsymbol{x}) - \hat{\boldsymbol{f}}(\boldsymbol{x},\boldsymbol{\theta}) &= \boldsymbol{f}(\boldsymbol{x}) - \hat{\boldsymbol{f}}(\boldsymbol{x},\boldsymbol{\theta}^*) + \hat{\boldsymbol{f}}(\boldsymbol{x},\boldsymbol{\theta}^*) - \hat{\boldsymbol{f}}(\boldsymbol{x},\boldsymbol{\theta}) \\ &= \boldsymbol{\varepsilon} + \tilde{\boldsymbol{\theta}}^{\mathrm{T}}\boldsymbol{\xi}(\boldsymbol{x})\end{aligned}$$

where $\tilde{\boldsymbol{\theta}} = \hat{\boldsymbol{\theta}} - \boldsymbol{\theta}^*$.

Assumption If the robot closed-loop system satisfies the following conditions:

Existing $c > 0$ satisfied by

$$[\boldsymbol{e} \quad \dot{\boldsymbol{e}}]^{\mathrm{T}} \in L_v(c) = \left\{\begin{bmatrix}\boldsymbol{e}\\ \dot{\boldsymbol{e}}\end{bmatrix}: \begin{bmatrix}\boldsymbol{e}\\ \dot{\boldsymbol{e}}\end{bmatrix}^{\mathrm{T}}\boldsymbol{P}\begin{bmatrix}\boldsymbol{e}\\ \dot{\boldsymbol{e}}\end{bmatrix} \leqslant c\right\} \Rightarrow |\ddot{\boldsymbol{q}}_{di} - \boldsymbol{k}_{vi}\dot{\boldsymbol{e}} - \boldsymbol{k}_{pi}\boldsymbol{e}| \leqslant \boldsymbol{u}_{i,\max},\ i = 1,2,\cdots$$

where $\boldsymbol{k}_{pi}$ and $\boldsymbol{k}_{vi}$ are row vectors of matrices $\boldsymbol{k}_p$ and $\boldsymbol{k}_v$, respectively; $L_v(c)$ is the estimated ellipsoid invariant set of the system stability attraction domain[20], and c is its radius; $\boldsymbol{u}_{i,\max}$ is the maximum output amplitude of each manipulator.

$[\boldsymbol{e}(0) \quad \dot{\boldsymbol{e}}(0)]^{\mathrm{T}}$ satisfying $[\boldsymbol{e}(0) \quad \dot{\boldsymbol{e}}(0)]^{\mathrm{T}} \in L_v(c)$.

In this case, the trajectory of the closed-loop system leading at $L_v(c)$ asymptotically converges to the origin. For any reference input $\boldsymbol{q}_d$ and any initial state $(\boldsymbol{q}(0) \quad \dot{\boldsymbol{q}}(0))$ satisfying $[\boldsymbol{e}(0) \quad \dot{\boldsymbol{e}}(0)]^{\mathrm{T}} \in L_v(c)$, the trajectory leading from $(\boldsymbol{q}(0) \quad \dot{\boldsymbol{q}}(0))$ will asymptotically converge to $(\boldsymbol{q}_d(t) \quad \dot{\boldsymbol{q}}_d(t))$.

Choosing a Lyapunov function candidate:

$$\boldsymbol{V} = \frac{1}{2}\boldsymbol{x}^{\mathrm{T}}\boldsymbol{P}\boldsymbol{x} + \frac{1}{2\gamma}\|\tilde{\boldsymbol{\theta}}\|^2, \gamma > 0$$

where $\boldsymbol{P}$ is symmetric and positive definite matrix, and satisfying the following Lyapunov equation:

$$\begin{bmatrix}0 & \boldsymbol{I}\\ -\boldsymbol{k}_p & -\boldsymbol{k}_v\end{bmatrix}^{\mathrm{T}}\boldsymbol{P} + \boldsymbol{P}\begin{bmatrix}0 & \boldsymbol{I}\\ -\boldsymbol{k}_p & -\boldsymbol{k}_v\end{bmatrix} = -\boldsymbol{Q}$$

where $\boldsymbol{Q}$ is positive definite matrix.

Combining Eqs(1), (3), (5), (6) with the feedback linearization function, the closed-loop system can be expressed as

$$\frac{\mathrm{d}}{\mathrm{d}t}\begin{bmatrix}\boldsymbol{e}\\ \dot{\boldsymbol{e}}\end{bmatrix} = \begin{bmatrix}0 & \boldsymbol{I}\\ -\boldsymbol{k}_p & -\boldsymbol{k}_v\end{bmatrix}\begin{bmatrix}\boldsymbol{e}\\ \dot{\boldsymbol{e}}\end{bmatrix} + \boldsymbol{B}[sat_h(\ddot{\boldsymbol{q}}_d - \boldsymbol{k}_v\dot{\boldsymbol{e}} - \boldsymbol{k}_p\boldsymbol{e} - \boldsymbol{\rho}(\boldsymbol{e})\boldsymbol{B}^{\mathrm{T}}\boldsymbol{P}\begin{bmatrix}\boldsymbol{e}\\ \dot{\boldsymbol{e}}\end{bmatrix}) + \boldsymbol{\varepsilon} + \tilde{\boldsymbol{\theta}}^{\mathrm{T}}\boldsymbol{\xi}(\boldsymbol{x}) - \ddot{\boldsymbol{q}}_d + \boldsymbol{k}_v\dot{\boldsymbol{e}} + \boldsymbol{k}_p\boldsymbol{e}] \quad (7)$$

The time derivative of the Lyapunov function $\boldsymbol{V}$ along the closed-loop Eq. (7) is given by

$$\begin{aligned}\dot{V} &= -\frac{1}{2}\boldsymbol{x}^{\mathrm{T}}\boldsymbol{Q}\boldsymbol{x} + \boldsymbol{x}^{\mathrm{T}}\boldsymbol{P}\boldsymbol{B}[sat_h(\ddot{\boldsymbol{q}}_d - \boldsymbol{k}_v\dot{\boldsymbol{e}} - \boldsymbol{k}_p\boldsymbol{e} - \boldsymbol{\rho}(\boldsymbol{e})\boldsymbol{B}^{\mathrm{T}}\boldsymbol{P}\begin{bmatrix}\boldsymbol{e}\\ \dot{\boldsymbol{e}}\end{bmatrix}) - \ddot{\boldsymbol{q}}_d + \boldsymbol{k}_v\dot{\boldsymbol{e}} + \boldsymbol{k}_p\boldsymbol{e}] \\ &\quad - \boldsymbol{\xi}^{\mathrm{T}}(\boldsymbol{x})\tilde{\boldsymbol{\theta}}\boldsymbol{B}^{\mathrm{T}}\boldsymbol{P}\boldsymbol{x} + \boldsymbol{\eta}^{\mathrm{T}}\boldsymbol{B}^{\mathrm{T}}\boldsymbol{P}\boldsymbol{x} + \frac{1}{\gamma}tr(\dot{\tilde{\boldsymbol{\theta}}}^{\mathrm{T}}\tilde{\boldsymbol{\theta}}) \\ &= -\frac{1}{2}\boldsymbol{x}^{\mathrm{T}}\boldsymbol{Q}\boldsymbol{x} + \sum_{i=1}^{n}\boldsymbol{v}_i[sat_{h,i}(\boldsymbol{k}_i - \boldsymbol{\rho}_i(\boldsymbol{e})\boldsymbol{v}_i) - \boldsymbol{k}_i] - \boldsymbol{\xi}^{\mathrm{T}}(\boldsymbol{x})\tilde{\boldsymbol{\theta}}\boldsymbol{B}^{\mathrm{T}}\boldsymbol{P}\boldsymbol{x} + \boldsymbol{\eta}^{\mathrm{T}}\boldsymbol{B}^{\mathrm{T}}\boldsymbol{P}\boldsymbol{x} \\ &\quad + \frac{1}{\gamma}tr(\dot{\tilde{\boldsymbol{\theta}}}^{\mathrm{T}}\tilde{\boldsymbol{\theta}})\end{aligned}$$

where $\boldsymbol{v}_i$ is the ith element of $\boldsymbol{B}^{\mathrm{T}}\boldsymbol{P}\begin{bmatrix}\boldsymbol{e}\\ \dot{\boldsymbol{e}}\end{bmatrix}$, and $\boldsymbol{k}_i = \ddot{\boldsymbol{q}}_{di} - \boldsymbol{k}_{vi}\dot{\boldsymbol{e}} - \boldsymbol{k}_{pi}\boldsymbol{e}$, $i = 1,2\cdots n$.

Considering item $\sum_{i=1}^{n}\boldsymbol{v}_i[sat_{h,i}(\boldsymbol{k}_i - \boldsymbol{\rho}_i(\boldsymbol{e})\boldsymbol{v}_i) - \boldsymbol{k}_i]$, for each robot manipulator, if $|\boldsymbol{k}_i - \boldsymbol{\rho}_i(\boldsymbol{e})\boldsymbol{v}_i| \leqslant \boldsymbol{u}_{i,\max}$, induces:

$$\boldsymbol{v}_i[sat_{h,i}(\boldsymbol{k}_i - \boldsymbol{\rho}_i(\boldsymbol{e})\boldsymbol{v}_i) - \boldsymbol{k}_i] = -\boldsymbol{\rho}_i(\boldsymbol{e})\boldsymbol{v}_i^2 \leqslant 0;$$

while $|\boldsymbol{k}_i - \boldsymbol{\rho}_i(\boldsymbol{e})\boldsymbol{v}_i| > \boldsymbol{u}_{i,\max}$, gives rise to $|\boldsymbol{k}_i| \leqslant \boldsymbol{u}_{\max}$.

Therefore,

$$\begin{cases}0 < sat_{h,i}(\boldsymbol{k}_i - \boldsymbol{\rho}_i(\boldsymbol{e})\boldsymbol{v}_i) - \boldsymbol{k}_i < -\boldsymbol{\rho}_i(\boldsymbol{e})\boldsymbol{v}_i, & \boldsymbol{k}_i > \boldsymbol{u}_{i,\max} \\ -\boldsymbol{\rho}_i(\boldsymbol{e})\boldsymbol{v}_i < sat_{h,i}(\boldsymbol{k}_i - \boldsymbol{\rho}_i(\boldsymbol{e})\boldsymbol{v}_i) - \boldsymbol{k}_i < 0, & \boldsymbol{k}_i < -\boldsymbol{u}_{i,\max}\end{cases}$$

It makes $\boldsymbol{v}_i$ and $sat_{h,i}(\boldsymbol{k}_i - \boldsymbol{\rho}_i(\boldsymbol{e})\boldsymbol{v}_i) - \boldsymbol{k}_i$ have opposite signs, indicating that:

$$\boldsymbol{v}_i[sat_{h,i}(\boldsymbol{k}_i - \boldsymbol{\rho}_i(\boldsymbol{e})\boldsymbol{v}_i) - \boldsymbol{k}_i] \leqslant 0.$$

always having

$$\sum_{i=1}^{n}\boldsymbol{v}_i[sat_{h,i}(\boldsymbol{k}_i - \boldsymbol{\rho}_i(\boldsymbol{e})\boldsymbol{v}_i) - \boldsymbol{k}_i] \leqslant 0,$$

which suggests for

$$\dot{V} \leqslant -\frac{1}{2}\boldsymbol{x}^{\mathrm{T}}\boldsymbol{Q}\boldsymbol{x} - \boldsymbol{\xi}^{\mathrm{T}}(\boldsymbol{x})\tilde{\boldsymbol{\theta}}\boldsymbol{B}^{\mathrm{T}}\boldsymbol{P}\boldsymbol{x} + \boldsymbol{\varepsilon}^{\mathrm{T}}\boldsymbol{B}^{\mathrm{T}}\boldsymbol{P}\boldsymbol{x} + \frac{1}{\gamma}tr(\dot{\tilde{\boldsymbol{\theta}}}^{\mathrm{T}}\tilde{\boldsymbol{\theta}})$$

note that $\boldsymbol{\xi}^{\mathrm{T}}(\boldsymbol{x})\tilde{\boldsymbol{\theta}}\boldsymbol{B}^{\mathrm{T}}\boldsymbol{P}\boldsymbol{x} = tr[\boldsymbol{B}^{\mathrm{T}}\boldsymbol{P}\boldsymbol{x}\boldsymbol{\xi}^{\mathrm{T}}(\boldsymbol{x})\tilde{\boldsymbol{\theta}}]$, and $\dot{\tilde{\boldsymbol{\theta}}} = \dot{\hat{\boldsymbol{\theta}}}$, so:

$$\dot{V} \leqslant -\frac{1}{2}\boldsymbol{x}^{\mathrm{T}}\boldsymbol{Q}\boldsymbol{x} + \boldsymbol{\varepsilon}^{\mathrm{T}}\boldsymbol{B}^{\mathrm{T}}\boldsymbol{P}\boldsymbol{x} + \frac{1}{\gamma}tr(\dot{\tilde{\boldsymbol{\theta}}}^{\mathrm{T}}\tilde{\boldsymbol{\theta}} - \gamma\boldsymbol{B}^{\mathrm{T}}\boldsymbol{P}\boldsymbol{x}\boldsymbol{\xi}^{\mathrm{T}}(\boldsymbol{x})\tilde{\boldsymbol{\theta}}) \quad (8)$$

In the following sections, two adaptive laws will be chosen to design a new type of controller and perform simulation analysis on their respective control performance.

3 Simulation and results

3.1 Case 1: adaptive law 1

Adaptive law 1 is chosen as

$$\dot{\hat{\boldsymbol{\theta}}} = \gamma \boldsymbol{B}^{\mathrm{T}} \boldsymbol{P} \boldsymbol{x} \boldsymbol{\xi}(\boldsymbol{x}), \ \gamma > 0 \tag{9}$$

Since $\dot{\tilde{\boldsymbol{\theta}}} = \dot{\hat{\boldsymbol{\theta}}}$, according to Eq. (8) and Eq. (9), the following is got:

$$\dot{V} \leqslant -\frac{1}{2}\boldsymbol{x}^{\mathrm{T}}\boldsymbol{Q}\boldsymbol{x} + \boldsymbol{\varepsilon}^{\mathrm{T}}\boldsymbol{B}^{\mathrm{T}}\boldsymbol{P}\boldsymbol{x}$$

According to the properties of the F norm:

$$\dot{V} \leqslant -\frac{1}{2}\lambda_{\min}(\boldsymbol{Q}) \|\boldsymbol{x}\|^2 + \|\boldsymbol{x}\| \ \|\boldsymbol{\varepsilon}_0\| \lambda_{\max}(\boldsymbol{P})$$
$$= -\frac{1}{2}\|\boldsymbol{x}\| [\lambda_{\min}(\boldsymbol{Q}) \|\boldsymbol{x}\| - 2\|\boldsymbol{\varepsilon}_0\| \lambda_{\max}(\boldsymbol{P})]$$

To make $\dot{V} \leqslant 0$, the following identity needs to be satisfied:

$$\|\boldsymbol{x}\| \geqslant \|\boldsymbol{\varepsilon}_0\| \frac{2\lambda_{\max}(\boldsymbol{P})}{\lambda_{\min}(\boldsymbol{Q})}$$

Then, new controller 1 is simulated and designed by adaptive law 1. A two degree of freedom manipulator is used in the simulation and the dynamic Eq. (1) is expressed as

$$\begin{pmatrix} 3.46 + 2.4\cos(q_2) & 0.96 + 1.2\cos(q_2) \\ 0.96 + 1.2\cos(q_2) & 0.96 \end{pmatrix}\begin{pmatrix} \ddot{q}_1 \\ \ddot{q}_2 \end{pmatrix}$$
$$+ \begin{pmatrix} -1.2\sin(q_2)\dot{q}_2 & -1.2\sin(q_2)(\dot{q}_1 + \dot{q}_2) \\ 1.2\sin(q_2)\dot{q}_2 & 0 \end{pmatrix}\begin{pmatrix} \dot{q}_1 \\ \dot{q}_2 \end{pmatrix}$$
$$+ \begin{pmatrix} 2.5\cos(q_2) + 12\cos(q_1 + q_2) \\ 12\cos(q_1 + q_2) \end{pmatrix} = \begin{pmatrix} \tau_1 \\ \tau_2 \end{pmatrix} + \begin{pmatrix} F_1 \\ F_2 \end{pmatrix}$$

The control goal is to make the output q_1, q_2 of the double joint track the desired trajectories $q_1 = \sin t$ and $q_2 = \sin t$, respectively. The initial value of the adaptive fuzzy control law parameter is set as $\theta(0) = [-2, -1, 0, 1, 2]$ and $\gamma = 20$. Defining the membership function as

$$\mu_{A_i^l}(x_i) = \exp\left(-\left(\frac{x_i - \bar{x}_i^l}{\frac{\pi}{24}}\right)^2\right)$$

where A_i is NB; NS, ZO, PS, PB, and $\bar{x}_i^l$ are $\frac{-\pi}{6}$, $\frac{-\pi}{12}, 0, \frac{\pi}{12}, \frac{\pi}{6}$ respectively.

The desired position is

$$[q_1 \quad q_2 \quad q_3 \quad q_4]^{\mathrm{T}} = [0 \quad 0 \quad 1 \quad 1]^{\mathrm{T}}.$$

Considering the uncertainties of friction and disturbance as

$$\boldsymbol{F}(\boldsymbol{q}, \dot{\boldsymbol{q}}, \ddot{\boldsymbol{q}}) = \begin{pmatrix} 15\dot{q}_1 + 6\mathrm{sgn}(\dot{q}_1) + 0.05\sin(20t) \\ 15\dot{q}_2 + 6\mathrm{sgn}(\dot{q}_1) + 0.1\sin(20t) \end{pmatrix},$$

and choosing $\alpha = 3$, the nonlinear feedback portion is $\boldsymbol{\rho}(\boldsymbol{e}) = \mathrm{diag}(600e^{(-60|\dot{e}_1|)}, 1500e^{(-47|\dot{e}_2|)})$.

Consequently $\boldsymbol{h} = \begin{bmatrix} h_1 \\ h_2 \end{bmatrix} = \begin{bmatrix} 47.5 \\ 30 \end{bmatrix}$ is calculated by Ref. [20]. In this work, $|sat_m(\cdot)| = |sat_h(\cdot)|$, and assume $\boldsymbol{Q} = 50\boldsymbol{I}$ are set.

In order to avoid system driver saturation, $\boldsymbol{\tau}(0) = \boldsymbol{M}(0)\boldsymbol{u}_{\max} \leqslant \boldsymbol{\tau}_{\max}$ must be satisfied, where $\boldsymbol{u}_{\max}$ is the maximum saturation value allowed by the composite nonlinear feedback control. After calculation, $\boldsymbol{u}_{\max} = \begin{bmatrix} \boldsymbol{u}_{1,\max} \\ \boldsymbol{u}_{2,\max} \end{bmatrix} = \begin{bmatrix} 100 \\ 50 \end{bmatrix}$ can be obtained.

The simulation results are shown in Fig. 1 – Fig. 3. Fig. 1(a) and Fig. 1(b) show the trajectory tracking of two robot joints under the control of each controller. When there are uncertainties in the robot system, the system control performance under the control of the original CNF controller is poor, and it no longer has the ability to track accurately. Although the tracking result under the control of adaptive fuzzy controller is better than the original CNF controller, there is a large overshoot and error in the tracking process. The adjustment time is long and the control performance needs to be improved. The uncertain robot system under new controller 1 has a rapid response, a small overshoot, a short adjustment time, a good precision tracking capability, and a superior control performance.

Fig. 2 and Fig. 3 show the torque estimation compensation and error generated by the adaptive fuzzy compensator for the uncertain term. It can estimate and compensate the torque generated by the uncertain items online, but the compensation error is relatively large, which is not conductive to improve the control performance of the system.

3.2 Case 2: adaptive law 2

Adaptive law 2 is chosen as

$$\dot{\hat{\boldsymbol{\theta}}} = \gamma \boldsymbol{B}^{\mathrm{T}} \boldsymbol{P} \boldsymbol{x} \boldsymbol{\xi}(\boldsymbol{x}) + k_1 \gamma \|\boldsymbol{x}\| \hat{\boldsymbol{\theta}}, \ \gamma, \ k_1 > 0 \tag{10}$$

Substituting Eq. (10) into Eq. (8), it can be obtained:

$$\dot{V} \leqslant -\frac{1}{2}\boldsymbol{x}^{\mathrm{T}}\boldsymbol{Q}\boldsymbol{x} + \boldsymbol{\varepsilon}^{\mathrm{T}}\boldsymbol{B}^{\mathrm{T}}\boldsymbol{P}\boldsymbol{x} + \frac{1}{\gamma}tr(k_1\gamma\|\boldsymbol{x}\|\hat{\boldsymbol{\theta}}^{\mathrm{T}}\tilde{\boldsymbol{\theta}})$$
$$= -\frac{1}{2}\boldsymbol{x}^{\mathrm{T}}\boldsymbol{Q}\boldsymbol{x} + \boldsymbol{\varepsilon}^{\mathrm{T}}\boldsymbol{B}^{\mathrm{T}}\boldsymbol{P}\boldsymbol{x} + k_1\|\boldsymbol{x}\| tr(\hat{\boldsymbol{\theta}}^{\mathrm{T}}\tilde{\boldsymbol{\theta}})$$

According to the properties of the F norm, $tr[\tilde{\boldsymbol{x}}^{\mathrm{T}}(\boldsymbol{x} - \tilde{\boldsymbol{x}})] \leqslant \|\tilde{\boldsymbol{x}}\|_F \|\boldsymbol{x}\|_F - \|\tilde{\boldsymbol{x}}\|_F^2$, then

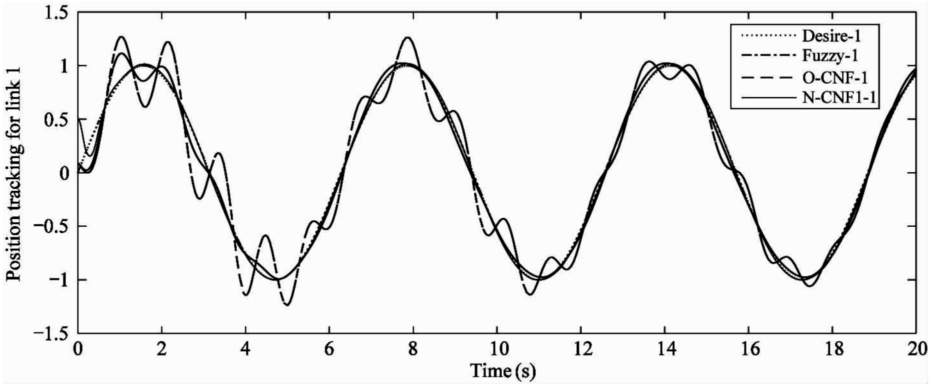

(a) Trajectory tracking results for joint 1

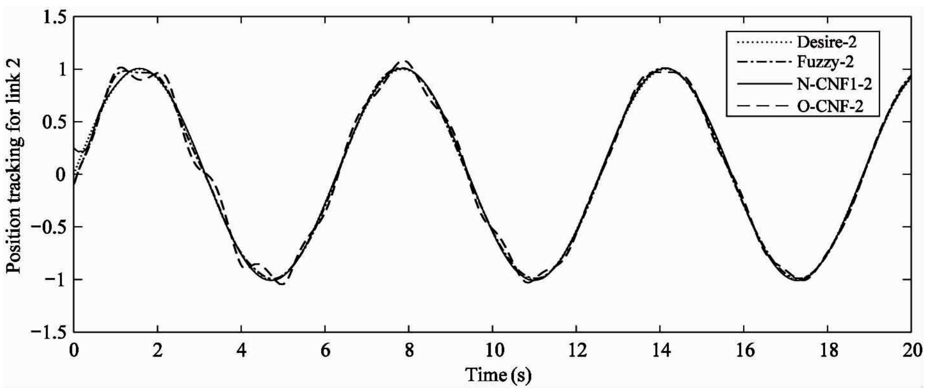

(b) Trajectory tracking results for joint 2

Fig. 1 Trajectory tracking results for joints (case 1)

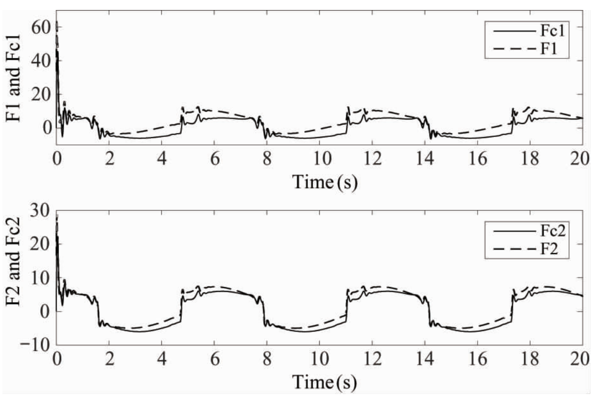

Fig. 2 Uncertainty estimation and its compensation (case 1)

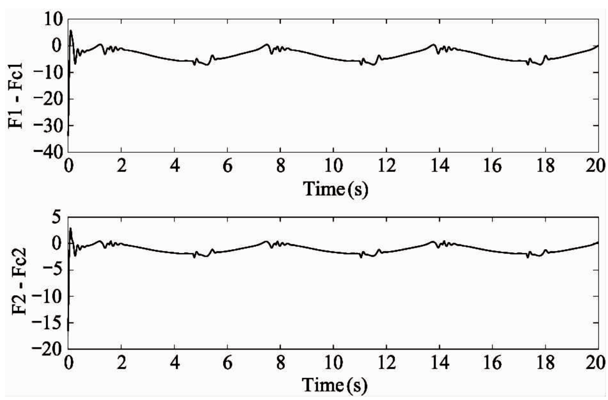

Fig. 3 Uncertainty estimation and compensation error (case 1)

$$
\begin{aligned}
\dot{V} &\leqslant -\frac{1}{2}\boldsymbol{x}^{\mathrm{T}}\boldsymbol{Q}\boldsymbol{x} + k_1 \|\boldsymbol{x}\| (\|\tilde{\boldsymbol{\theta}}_F\| \boldsymbol{\theta}^* \|_F \\
&\quad - \|\tilde{\boldsymbol{\theta}}\|_F^2) + \boldsymbol{\varepsilon}^{\mathrm{T}}\boldsymbol{B}^{\mathrm{T}}\boldsymbol{P}\boldsymbol{x} \\
&\leqslant - \|\boldsymbol{x}\| [\frac{1}{2}\lambda_{\min}(\boldsymbol{Q}) + k_1(\|\tilde{\boldsymbol{\theta}}\|_F - \frac{\boldsymbol{\theta}_{\max}}{2})^2 \\
&\quad - \frac{k_1}{4}\boldsymbol{\theta}_{\max}^2 - \|\boldsymbol{\varepsilon}_0\| \lambda_{\max}(\boldsymbol{P})]
\end{aligned}
$$

To make $\dot{V} \leqslant 0$, the following identity needs to be satisfied:

$$
\frac{1}{2}\lambda_{\min}(\boldsymbol{Q}) \|\boldsymbol{x}\| \geqslant \frac{k_1}{4}\boldsymbol{\theta}_{\max}^2 + \|\boldsymbol{\varepsilon}_0\| \lambda_{\max}(\boldsymbol{P})
$$

It means that the convergence condition is

$$
\|\boldsymbol{x}\| \geqslant \frac{2}{\lambda_{\min}(\boldsymbol{Q})}\left(\frac{k_1}{4}\boldsymbol{\theta}_{\max}^2 + \|\boldsymbol{\varepsilon}_0\| \lambda_{\max}(\boldsymbol{P})\right)
$$

Compared with adaptive law 1, adaptive law 2 can ensure the boundedness of the parameters, i. e, to solve the convergence problem of the adaptive fuzzy control system. Obviously, a smaller convergence value of $\boldsymbol{x}$ can be ensured by using a small eigenvalue of matrix $\boldsymbol{P}$, a smaller upper bound $\boldsymbol{\varepsilon}_0$ of the modeling error , and a smaller $\boldsymbol{\theta}_{\max}$, leading to a better tracking effect.

The simulation and analysis of new controller 2 also use the robot model of Section 3. 1. The simulation results are shown in Fig. 4 – Fig. 6. Fig. 4(a) and Fig. 4(b) are trajectory tracking results of 2 controllers for each robot joint. Compared with adaptive law 1, this new controller has smaller overshoot and less error, shorter adjustment time and better tracking effect when tracking the trajectory of an uncertain robot.

Fig. 5 and Fig. 6 are torque estimation compensation and error generated by the uncertain term. Compared with Fig. 2 and Fig. 3, it can estimate and compensate for the torque generated by the uncertain items online more accurately. Although it can be seen from Fig. 6 that the instantaneous compensation error is large at some time, but the saturation function in the new controller can effectively suppress the influence of the larger compensation error on the system at this time, as shown in Fig. 4.

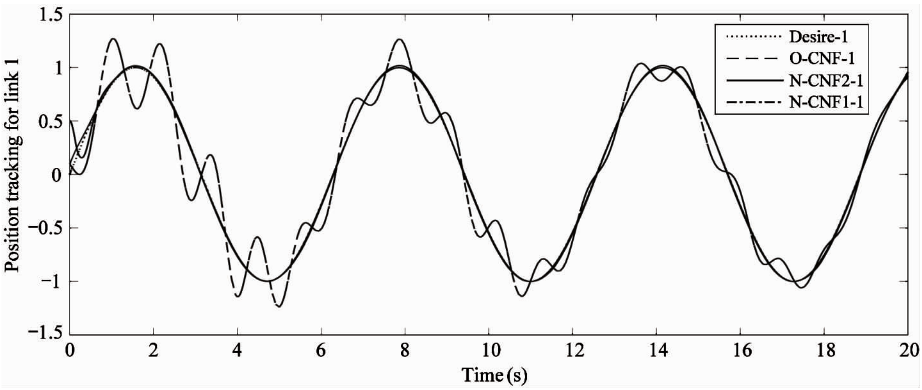

(a) Trajectory tracking results for joint 1

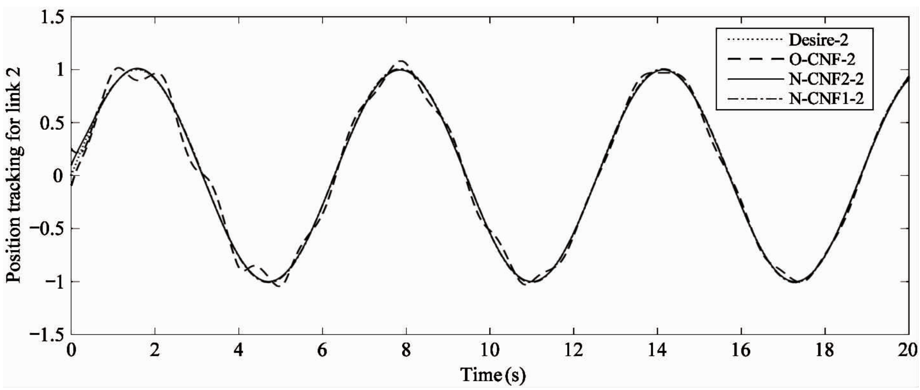

(b) Trajectory tracking results for joint 2

Fig. 4 Trajectory tracking results for joints (Case 2)

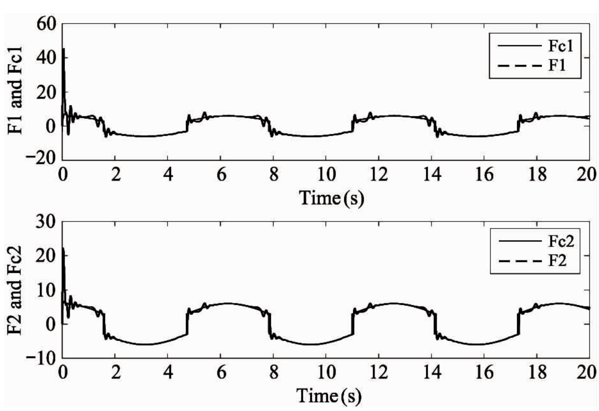

Fig. 5 Uncertainty estimation and its compensation (Case 2)

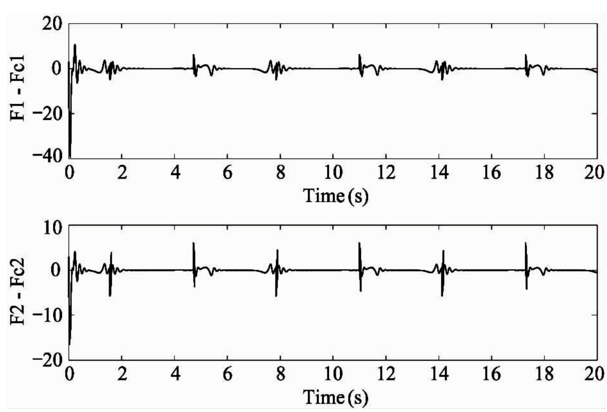

Fig. 6 Uncertainty estimation and compensation error (Case 2)

It can be seen from Fig. 7 that the control input of the two new controllers is more smooth and stable than the original controller. It can provide a continuous and stable control torque for the uncertain system, and guarantee the superior control performance of the uncertain system. Compared with the two new controllers, new controller 2 has better control performance, and provides a more stable and smooth control input for the system. Its superior control performance can also be seen from Fig. 4 – Fig. 6.

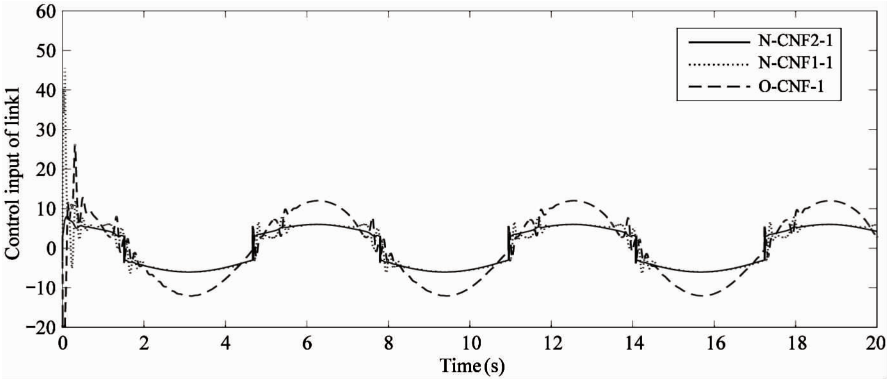

(a) The control input of joint 1

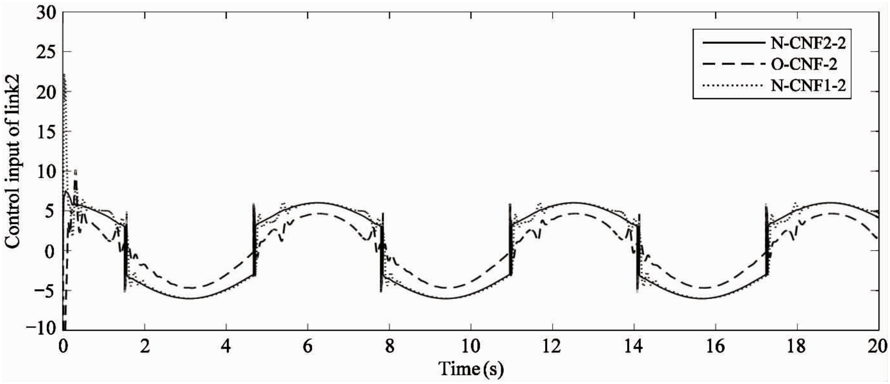

(b) The control input of joint 2

Fig. 7 Control input of 2 joints

4 Conclusion

The adaptive fuzzy control is used to approach the uncertain model of the robot online, and a composite nonlinear feedback controller based on adaptive fuzzy compensation is formed. By comparing the control performance of the new controller designed by 2 adaptive laws, an adaptive law that is relatively suitable for the uncertain robot system is selected. The design of fuzzy adaptive compensator is independent of the original system. The introduction of adaptive fuzzy compensator has no effect on the design of the original system. It is proved that the new controller can not only achieve good tracking performance, but also have good robustness and stability. This new controller not only retains the advantages of fast response, small overshoot, and effective suppression of system jitter of the CNF controller, but also preserves the advantages of the adaptive fuzzy controller for effective estimation of system uncertainties and rapid convergence. Therefore, the scheme can be extended to the space tracking task of robot manipulators.

References

[1] Liu J K. Design of Robot Control System and Matlab Simulation[M]. Beijing: Tsinghua University Press, 2017: 92-102 (In Chinese)

[2] Aflakiyan A, Bayani H, Masouleh M T. Computed torque control of a cable suspended parallel robot[C]//Proceedings of the 2016 4th RSI/ISM International Conference on Robotics and Mechatronics (ICRoM), Tehran, Iran, 2016: 749-754

[3] Yin G, Zhang X, Chen J, et al. Trajectory tracking adaptive control of the lower limb rehabilitation robot with model uncertainty[J]. *Journal of Electronic Measurement and Instrumentation*, 2016, 68(6): 387-395

[4] Sadati N, Babazadeh A. Optimal control of robot manipulators with a new two-level gradient-based approach[J]. *Electrical Engineering*, 2006, 88(5):383-393

[5] Siciliano B, Sciavicco L. Modelling and control of robot manipulators[J]. *Industrial Robot*, 2005, 11(1):1828-1833

[6] Reham H, Bendary F, Elserafi K. Trajectory tracking control for robot manipulator using fractional order-fuzzy-PID controller[J]. *International Journal of Computer Applications*, 2016, 134(15): 22-29

[7] Li X, Chen C C. Adaptive neural network control of robot based on a unified objective bound[J]. *IEEE Transactions on Control Systems Technology*, 2013, 22(3):1032-1043

[8] Liu K, Xu J, Ge Z, et al. Robust control of 3-DOF parallel robot driven by PMAs based on nominal stiffness model[J]. *Advanced Robotics*, 2017, 31(10):531-543

[9] Zhao L M. Research on Robot Control Uncertainty and Saturated Attraction Domain Evaluation[D]. Shanghai: Department of Automation, Shanghai Jiaotong University, 2008: 45-49 (In Chinese)

[10] Liu Y, Gao X, Dai F. Implementation of mamdami fuzzy control on a multi-DOF two-wheel inverted pendulum robot[J]. *Discrete and Continuous Dynamical Systems-Series S (DCDS-S)*, 2017, 8(6):1251-1266

[11] He W, Dong Y. Adaptive fuzzy neural network control for a constrained robot using impedance learning[J]. *IEEE Transactions on Neural Networks and Learning Systems*, 2017, 29(4):1174-1186

[12] Yang J, Su H, Li Z, et al. Adaptive control with a fuzzy tuner for cable-based rehabilitation robot[J]. *International Journal of Control Automation and Systems*, 2016, 14(3):865-875

[13] Abdelhamid B, Mouhamed C, Najib E. Indirect robust adaptive fuzzy control of uncertain two link robot manipulator[C]//Proceedings of the 3rd International Conference on Electrical Engineering and Control Applications, Constantine, Algeria, 2017: 125-139

[14] Lin Z, Pachter M, Banda S. Toward improvement of tracking performance nonlinear feedback for linear systems[J]. *International Journal of Control*, 1998, 70(1): 1-11

[15] Chen B M, Lee T H, Peng K, et al. Composite nonlinear feedback control for linear systems with input saturation: theory and an application[J]. *IEEE Transactions on Automatic Control*, 2002, 48(3):427-439

[16] Wang N, Er M J, Sun J C, et al. Adaptive robust online constructive fuzzy control of a complex surface vehicle system[J]. *IEEE Transactions on Cybernetics*, 2017, 46(7):1511-1523

[17] He W, Chen Y, Yin Z. Adaptive neural network control of an uncertain robot with full-state constraints[J]. *IEEE Transactions on Cybernetics*, 2016, 46(3):620-629

[18] Peng W D, Su J B. Robot control method based on combined nonlinear feedback technology [J]. *Chinese High Technology Letters*, 2010, 19(6):591-595 (In Chinese)

[19] Yahiaoui F, Guenounou O, Brikh L, et al. Maximum power point tracking algorithm for photovoltaic system using a PSO optimized fuzzy logic controller[C]//Proceedings of the 3th International Conference on Green Energy and Environmental Engineering, Sousse, Tunisia, 2016: 304-310

[20] Peng W D. Composite nonlinear feedback controller for robot manipulators with bounded torques[D]. Shanghai: Department of Automation, Shanghai Jiaotong University, 2009: 39-59 (In Chinese)

Jiang Yuan, born in 1982. He received his Ph. D degree in control theory and control engineering from Shandong University in 2010. He also received his B. S. degree from Changsha University of Science and Technology in 2004, and received his M. S. degree from Guangxi Teachers Education University in 2007. Now, he is an assciate professor in School of Information Engineering, Nanchang Hangkong University, China. He visited the University of Chinese Academy of Sciences as a Visiting Scholar in 2019. His research interests include nonlinear and adaptive control design, disturbance rejection, output regulation, flight control of helicopter.